JACS
JOURNAL OF THE AMERICAN CHEMICAL SOCIETY
Article
Cite This: J. Am. Chem. Soc. 2019, 141, 8503−8508
pubs.acs.org/JACS

Abnormally Strong Electron−Phonon Scattering Induced Unprecedented Reduction in Lattice Thermal Conductivity of Two-Dimensional Nb_2C

Yongda Huang, Jian Zhou, Guanjie Wang, and Zhimei Sun*

School of Materials Science and Engineering, Beihang University, Beijing 100191, China

Center for Integrated Computational Materials Engineering, International Research Institute for Multidisciplinary Science, Beihang University, Beijing 100191, China

Supporting Information

ABSTRACT: In most materials the electron−phonon (e-p) scattering is far weaker than phonon−phonon (p-p) scattering, and the e-p scattering is usually proportional to the e-p coupling strength. Here, we report strong e-p scattering but low e-p coupling strength in two-dimensional(2D) Nb_2C by first-principles calculations. Moreover, the intensity of e-p scattering is close to that of p-p scattering at 300 K in sharp contrast to normal cases. This abnormal e-p scattering is understood by a specific feature that the energy difference between occupied and empty electron states near the Fermi level is in the order of the characteristic phonon energy. By calculating the phonon transport property of 2D Nb_2C, we show that this strong e-p scattering can result in great reduction in the lattice thermal conductivity.Our work also highlights a new way for searching novel 2D materials with low lattice thermal conductivity.

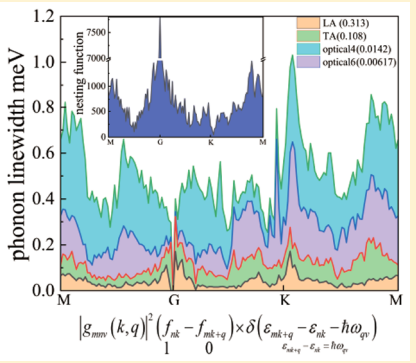

INTRODUCTION

Phonon transport property has profound influences on the performance of electronic devices. The lattice thermal conductivity is the common physical quantity to represent the phonon transport that determined by electron−phonon (e-p) scattering and phonon−phonon (p-p) scattering. In the early years, the e-p scattering was not considered in the calculation of lattice thermal conductivity.[1−5] Recently, it has been shown that the different magnitudes of e-p scattering have important sizable effects on the phonon transport by first-principles calculations.[6−10] This is attributed to the phonon self-energy which is the electron−phonon scattering form that influences the phonon transport property. The phonon self-energy will lead to significant renormalization of the phonon.[11] Some experiments have been explored to understand the phonon self-energy effect,[12] among which the most important work is the giant phonon self-energy effect observed in layered MgB_2 by Raman spectroscopy.[13] Nevertheless, for 2D metallic materials, no progress has been made by first-principles calculations with many-body physics analysis so far.

Theoretically the strong e-p scattering is more likely to occur in 2D metallic materials due to enough density of electron states near the Fermi energy. Experimentally strong e-p scattering is possible to induce high photothermal conversion efficiency due to the increased quantity of the heat caused by the collision between photon and phonon. Recently, 2D Nb_2C has been investigated for the application in the photothermal tumor eradication due to its high photothermal conversion efficiency.[14] 2D Nb_2C belongs to a large family of two-dimensional transition metal carbides[15−17] and is a good metallic conductor. Moreover, 2D Nb_2C has also been studied to have potential applications as electrode materials for supercapacitors[18] and photocatalysts for hydrogen evolution.[19,20] Based on the high photothermal conversion efficiency properties of 2D Nb_2C, we speculate that Nb_2C could exhibit strong e-p scattering rate. In this work, we have implemented the strong e-p scattering effect in the phonon transport calculations by first-principles, and then using this technique we have calculated the phonon transport property for 2D Nb_2C. In stark contrast to normal cases, in 2D Nb_2C the intensity of e-p scattering is close to that of p-p scattering at 300 K, even though the e-p coupling strength is rather small. Further, the strong electron−phonon scattering induced great reduction in the lattice thermal conductivity of 2D Nb_2C. Our results may offer a new perspective to the effect of the electron−phonon interaction.

We used the Quantum ESPRESSO package 6.2.1(QE)[21] and the Vienna Ab initio Simulation Package (VASP)[22] for the density functional theory and density functional perturbation theory calculations with a norm-conserving pseudopotential with the Perdew−Burke−Ernzerhof exchange-correlation functional. The VASP+ShengBTE[23] is used to get the lattice thermal conductivity data of phonon−phonon interaction and the QE+EPW (Electron−Phonon-Wannier)[24] is used to calculate the electron−phonon matrix to get electron−phonon

Received: February 15, 2019
Published: May 6, 2019

DOI: 10.1021/jacs.9b01742
J. Am. Chem. Soc. 2019, 141, 8503−8508

scattering rate due to the phonon self-energy. Methfessel–Paxton method[25] and 30 × 30 × 1 kpoints are chosen to ensure the convergence in EPW. Due to the limit of DFPT (density functional perturbation theory) algorithm, the ZA (Z-axis acoustic) phonon can not be calculated accurately.[26] However, it does not influence the property of TA (transverse acoustic) and LA (longitudinal acoustic) and the reduction effect of lattice thermal conductivity.

RESULTS AND DISCUSSION

As a first step to explore the phonon transport property, we have examined the structure stability. As illustrated in Figure 1a, no negative frequency is observed in the phonon spectrum

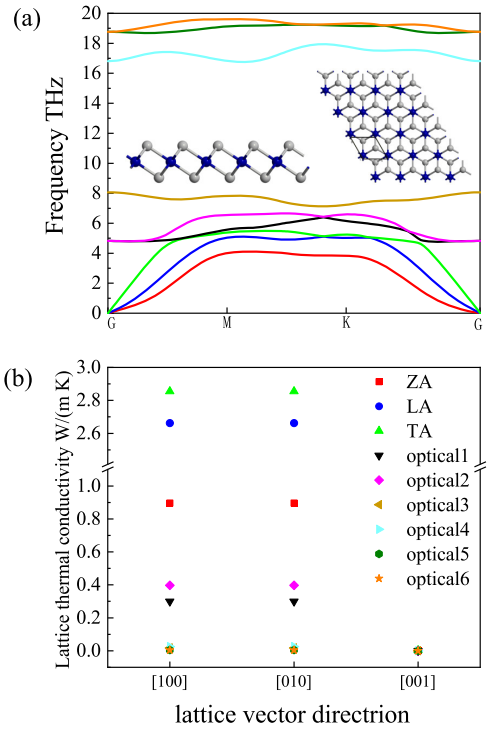

Figure 1. (a) Phonon spectrum and the structure of 2D Nb_2C. The phonon branches correspond to panel b. (b) Lattice thermal conductivity for phonon branches (300 K) in three directions [100], [010], and [001] without considering effective thickness.

of 2D Nb_2C, confirming its lattice stability. It is further noticed that there are nine phonon branches, including three acoustic branches and six optical branches. The contribution to the lattice thermal conductivity for these nine phonon branches is presented in Figure 1b. Remarkably, the lattice thermal conductivity of 2D Nb_2C is mainly contributed by the ZA, LA, and TA phonon branches in the directions of [100] and [010], while the other six optical branches have small contribution. On the other hand, due to the vacuum along the Z axis direction, the lattice thermal conductivity along [001] is close to 0. Therefore, in the following we will focus on the three acoustic branches.

Usually, the key to determine lattice conductivity is the p-p and e-p scattering processes. The phonon–phonon scattering rate is easy to calculate by ShengBTE. While the electron–phonon scattering is different. An e-p scattering equation can be introduced by the many-body field theory:[27,28]

$$\Omega_{q\nu}^{\ 2} \simeq \omega_{q\nu}^{\ 2} + 2\omega_{q\nu}\mathrm{Re}\Pi_{q\nu\nu'}^{\mathrm{NA}}(\omega_{q\nu}) \quad (1)$$

$$\gamma_{q\nu} \simeq -\frac{\omega_{q\nu}}{\Omega_{q\nu}}\mathrm{Im}\,\Pi_{q\nu\nu'}^{\mathrm{NA}}(\omega_{q\nu}) \quad (2)$$

Herein $\omega_{q\nu}$ is the phonon frequency without e-p coupling, $\Pi_{q\nu\nu'}^{\mathrm{NA}}(\omega_{q\nu})$ is the phonon self-energy, and $\Omega_{q\nu}$ is the phonon frequency with e-p coupling, that can be extracted directly from the phonon spectral function.[29] $\gamma_{q\nu}$ is the phonon linewidth, from which, we can get the electron–phonon scattering rate $\frac{1}{\tau_{e-p}}$ as $\gamma_{q\nu} = \frac{\hbar}{\tau_{e-p}}$,[30] where τ_{e-p} is the phonon lifetime due to e-p scattering.

The calculated average scattering rate for e-p and p-p as a function of temperature is shown in Figure 2. The different

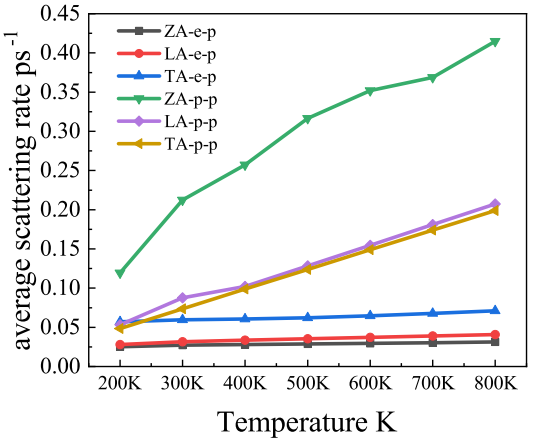

Figure 2. Scattering rate of ZA, LA, and TA for p-p and e-p at different temperatures.

scattering rate for various branches represents different responses to temperature. Obviously, the p-p scattering is enhanced with increasing the temperature, but there is negligible influence of temperature on the e-p scattering. In other words, the electron–phonon scattering rate of the three acoustic branches are insensitive to temperatures,[31] while the p-p scattering is sensitive to temperature. At the high temperatures the phonon–phonon scattering rate increase drastically and hence becomes the main contribution to the lattice thermal conductivity. It is also noted that the p-p scattering rate of the ZA branch is extremely large which originates from the character of the two-dimensional structure for Nb_2C. Due to the buckled structure of Nb_2C, symmetry-based phonon–phonon scattering selection rule is broken that results in a large p-p scattering rate of the out-of-plane ZA mode.[32] Nevertheless, since symmetry-based selection rule does not work in the e-p scattering, e-p scattering of ZA behaves differently from p-p scattering. The behavior of e-p scattering corresponding to different temperatures are similar and we will discuss that below eq 5. Again in Figure 2, it is noticed that at 800 K the p-p scattering is much larger than the e-p scattering, indicating that the e-p scattering effect can be ignored at high temperatures. At low temperatures especially at below 300 K the electron–phonon scattering rate is nearly as strong as the phonon–phonon scattering rate, in sharp contrast to the normal case that the latter is 100 times stronger than the former. To the best of our knowledge, this is the first time that a strong e-p scattering comparable to p-p scattering is found in two-dimensional metallic materials. Additionally, because the photothermal conversion efficiency is

DOI: 10.1021/jacs.9b01742
J. Am. Chem. Soc. 2019, 141, 8503–8508

related to the electron−phonon scattering rate, our present results also reveal that the experimentally reported phenomenon of high photothermal conversion efficiency in 2D Nb_2C should be due to the strong e-p scattering rate.

To unravel the physical origin of this unusual strong e-p scattering, it is natural to think of the parameter of e-p scattering strength, larger e-p coupling strength should produce stronger e-p scattering. In the present case, the electron−phonon coupling constants λ_{qv} is described as the quantity of electron−phonon interaction:[24]

$$\lambda_{qv} = \frac{1}{N(\varepsilon_F)\omega_{qv}} \sum_{nm} \int_{BZ} \frac{dk}{\Omega_{BZ}} \times |g_{mnv}(k, q)|^2 \delta(\varepsilon_{nk} - \varepsilon_F)\delta(\varepsilon_{mk+q} - \varepsilon_F) \quad (3)$$

where $g_{mnv}(k,q)$ is electron−phonon coupling matrix, electron band index m,n, phonon band index v. Also the summations are in the range of all band index. The calculated e-p coupling constants for the dominated three acoustic branches are ZA 0.175, LA 0.313, and TA 0.108, from which an average e-p coupling constant λ is estimated to be about 0.2. Clearly such a weak e-p coupling should not be the origin for the strong e-p scattering rate at below 300 K. We then resort to eq 2, it is obvious that the phonon self-energy is the primary physical quantity to control e-p scattering. The phonon self-energy at temperature T for metals can be calculated by first-principles within the many-body theory of electron−phonon coupling:[33]

$$\hbar\Pi^{NA}_{qvv}(\omega) = 2\sum_{mn} \int \frac{dk}{\Omega_{BZ}} g^{b}_{mnv}(k, q) g^{*}_{mnv}(k, q) \left[\frac{f_{mk+q} - f_{nk}}{\varepsilon_{mk+q} - \varepsilon_{nk} - \hbar(\omega + i\eta)} - \frac{f_{mk+q} - f_{nk}}{\varepsilon_{mk+q} - \varepsilon_{nk}} \right] \quad (4)$$

where $g^{b}_{mnv}(k,q)$ is bare electron−phonon matric element, $g^{*}_{mnv}(k,q)$ is the screened matrix element (Supporting Information). As eq 2 shows, the imaginary part of the phonon self-energy in eq 4 that is multiplied by $-\frac{\omega_{qv}}{\Omega_{qv}}$ is the e-p scattering rate. Equation 5 is obtained from replacing $g^{b}_{mnv}(k,q)$ $g^{*}_{mnv}(k,q)$ by the unscreening $|g_{mn,v}(k, q)|^2$:[29]

$$\frac{1}{\tau^{ph}_{qv}} = \frac{\omega_{qv}}{\Omega_{qv}} \frac{2\pi}{\hbar} 2\sum\nolimits_{mn} \int \frac{dk}{\Omega_{BZ}} |g_{mnv}(k, q)|^2 (f_{nk} - f_{mk+q}) \times \delta(\varepsilon_{mk+q} - \varepsilon_{nk} - \hbar\omega_{qv}) \quad (5)$$

where $g_{mnv}(k, q)$ is the electron−phonon coupling matrix, f_{nk} and f_{mk+q} is the Dirac-Fermi distribution, ε_{mk+q} and ε_{nk} are the electron energy, and ω_{qv} is the phonon frequency. According to eq 5, ignoring the constants term $\frac{\omega_{qv}}{\Omega_{qv}}$, $\frac{1}{\tau^{ph}_{qv}}$ can be large with weak electron−phonon coupling only when the following situation is satisfied: the empty single-particle states are separated by an energy in the order of the characteristic phonon energy. In other words, there are two electron states near the Fermi energy level, one occupied but the other empty. Meanwhile, the energy difference between these two electron states is the phonon eigenvalue energy. Moreover, eq 5 can be extended to finite temperature by simply replacing the occupation factors f_{nk} and f_{mk+q} by the Fermi−Dirac distributions of the corresponding temperature, and the Fermi−Dirac distribution is insensitive to temperature. Therefore, the e-p scattering of three acoustic branches have similar behavior respect to temperature. Furthermore, as the e-p scattering rate is proportional to the phonon linewidth, in the following we will analyze the phonon linewidth at 300 K in detail.

Figure 3 shows the calculated phonon linewidth for the LA, TA, optical4, and optical6 branches. Comparing the phonon

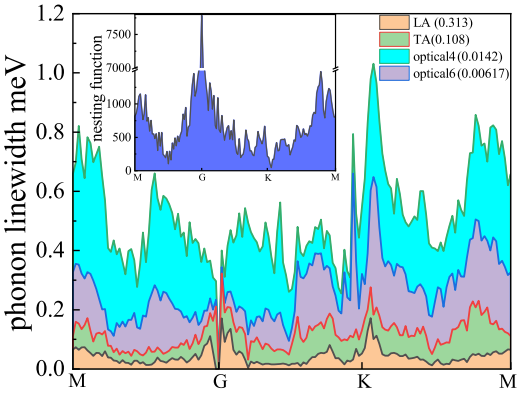

Figure 3. Phonon linewidth (ignoring constants term) of LA, TA, optical4, and optical6 with electron−phonon coupling constants of 0.313, 0.108, 0.0142, and 0.00617 and nesting function at 300 K.

linewidth with the corresponding λ values for these four branches, the optical6 and optical4 branches present larger phonon linewidth but smaller coupling constants than the LA and TA branches. To understand this, a simplified equation is introduced herein, i.e., when $T \rightarrow 0$, the condition that produces the large phonon linewidth by eq 5 can be written as[34]

$$|q \cdot v_F| \approx \omega \quad (6)$$

where v_F is the Fermi velocity, q is the phonon wave vector, and ω is the phonon frequency. This condition can be extended to the finite temperature qualitatively. Accordingly, the property of e-p scattering is related to the phonon frequency. Because the $|q \cdot v_F|$ is usually larger than the phonon frequency, a larger phonon frequency is easier to satisfy the condition of eq 6. Thus, the e-p scattering rate for the optical6 and optical4 branches is larger than the acoustic branches LA and TA. In addition, comparing the phonon frequency of optical4 with optical6, both of them belong to the high frequency phonon branches. In this case, the e-p coupling strength is decisive. So the larger e-p coupling strength of optical4 induces the larger phonon linewidth than optical6. This phenomenon emphasizes the greater importance of the phonon eigenvalue than e-p interaction strength in the e-p scattering process due to phonon self-energy. The Fermi nesting function calculated by eq 5 shown as an inset figure of Figure 3 can help to further confirm this conclusion.[35]

$$\zeta_q = \sum_{nm} \int_{BZ} \frac{dk}{\Omega_{BZ}} \delta(\varepsilon_{nk} - \varepsilon_F)\delta(\varepsilon_{mk+q} - \varepsilon_F) \quad (7)$$

where ε_{nk}, ε_{mk+q} is electron state energy and ε_F is Fermi energy. The nesting function is determined by the number of electron states and the magnitude of $\delta(\varepsilon_{nk} - \varepsilon_F)\delta(\varepsilon_{mk+q} - \varepsilon_F)$. A large nesting function demonstrates that enough electron states can easily jump from one state to another state over some phonon eigenvector around the Fermi surface.[36] Thus, it can qualitatively represent the degree of ease in the electron

DOI: 10.1021/jacs.9b01742
J. Am. Chem. Soc. 2019, 141, 8503−8508

transfer. The large nesting function can increase the possibility to find two electron states ε_{nk} and ε_{mk+q} around the Fermi energy that are separated by the phonon energy. So generally the larger nesting function can induce a larger phonon linewidth. Note that the gamma point has no phonon frequency, so this does not have any phonon linewidth. For K point, as the energy bands (Supporting Information) shown, the energy bands degenerate at around the K point of the Fermi energy, so the nesting function is small because there are less electron states participating in the transition process around K point. This also indicates that the large nesting function is the sufficient but unnecessary condition for leading to a large phonon linewidth.

Combining the above results and analysis, the general characters for strong electron−phonon scattering are concluded as follows: (1) enough electron states around the Fermi surface, (2) high phonon frequency, and (3) strong electron−phonon coupling. The importance of the three conditions is arranged in decreased orders. The first condition is the most important one, and it is also the reason that only metals and doped semiconductors have strong e-p scattering. The third condition is self-evident that stronger electron−phonon coupling gets stronger e-p scattering. The second condition makes phonon easily satisfy the condition of eq 5. In other words, higher phonon frequency means larger phonon energy ω_{qv} which make term $\delta(\varepsilon_{mk+q} - \varepsilon_{nk} - \omega_{qv})$ be larger. As the collision model of solid balls, higher frequency phonons are more likely to collide with electrons and the e-p coupling describes the strength of each collision. And our results show that high phonon frequency is more important than electron−phonon coupling strength.

Finally as the electron−phonon scattering exhibits strong effect, we calculate the lattice thermal conductivity considering e-p scattering. The lattice thermal conductivity can be calculated as the sum of contributions from all phonon modes:[37]

$$k = \frac{1}{3}\sum_{qv} C_{qv} v_{qv}^{\ 2} \tau_{qv} \tag{8}$$

where C_{qv} is the mode-specific heat capacity, v_{qv} is the group velocity, and τ_{qv} is the total lifetime. The critical calculation is the total lifetime τ_{qv}. Based on the Mattiessen rule,[38] we utilize the accurate self-consistent solution of Boltzmann equation[39,40] to calculate the total phonon lifetime:

$$\frac{1}{\tau} = \frac{1}{\tau^{\mathrm{e-p}}} + \frac{1}{\tau^{\mathrm{p-p}}_{\text{self-consistent-solution}}} \tag{9}$$

This method can be applied in a system that has strong electron−phonon scattering rate due to the phonon self-energy. We have calculated the thermal conductivity for 2D Nb_2C in the two thermal propagating directions of [100] and [001], the results of which are shown in Figure 4 where the inset figure is the enlarged view for the results in [100] with both p-p and e-p. Due to the structural symmetry of 2D Nb_2C, the lattice thermal conductivity is the same in the directions of [100] and [010], and the lattice thermal conductivity of [001] can be ignored. As is clearly seen in Figure 4, significant reduction in the lattice thermal conductivity is obtained when including the effect of electron−phonon scattering. That is to say, one should consider both e-p and p-p scattering when calculating the lattice thermal conductivity for metallic 2D materials Nb_2C, otherwise one will significantly overestimate

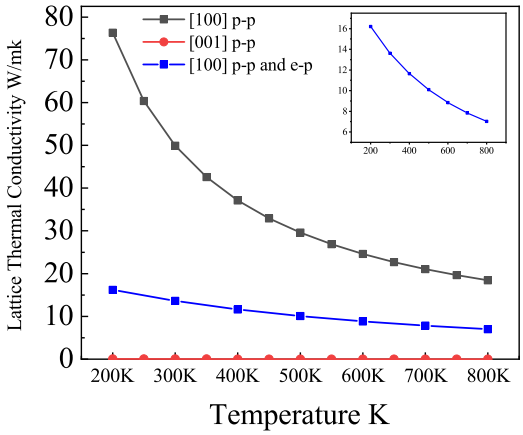

Figure 4. Lattice thermal conductivity considering the e-p and p-p scattering. The black and red lines are the lattice thermal conductivity considering only with p-p scattering. The blue line is the lattice thermal conductivity considered with both p-p and e-p scattering. (Here we have considered effective thickness).

the thermal conductivity if the e-p scattering was ignored. Actually, both the work of Pt and Ni[9] and that of NiAl and Ni3Al[10] reported strong e-p (electron−phonon) scattering and the mechanism was attributed to the strong e-p couplings with high electron density of states near the Fermi level. These two works satisfy the conventional case that the strong e-p scattering is induced by strong e-p coupling as we have stated before; that is, in most materials the e-p scattering is usually proportional to the e-p coupling strength. Unlike the conventional case, here we report that the strong e-p scattering exhibits an unusual weak e-p coupling strength in 2D Nb_2C. Furthermore, the work of 3D NbC[35] reported that large Fermi nesting function can induce strong electron−phonon scattering. However, our work clarified that the large nesting function is the sufficient but unnecessary condition for leading to a large electron−phonon scattering. Thus large Fermi nesting can not lead to the scattering rate inversion of TA (0.313) and LA (0.108) in 2D Nb_2C.

CONCLUSION

In conclusion, we have calculated the e-p scattering rate and p-p scattering rate for metallic 2D Nb_2C by first principles. Unlike most materials, the e-p scattering is nearly as strong as p-p scattering at below 300 K, even though the e-p coupling strength is small. We have also discussed the temperature effect on the e-p and p-p scattering; that is, the p-p scattering is more sensitive to temperatures while the e-p scattering is not. Due to this property, the materials that have strong e-p scattering could be applied as the stable thermal resistance components at low temperatures. Meanwhile, we have elaborately analyzed the mechanism for this unusual strong e-p scattering in 2D Nb_2C. Further, our calculated lattice thermal conductivity with e-p scattering unambiguously demonstrates that the strong e-p scattering can result in giant reduction in the lattice thermal conductivity. Last but not least, our present method and conclusion can be extended to other metallic 2D materials.

ASSOCIATED CONTENT

Supporting Information

The Supporting Information is available free of charge on the ACS Publications website at DOI: 10.1021/jacs.9b01742.

DOI: 10.1021/jacs.9b01742
J. Am. Chem. Soc. 2019, 141, 8503−8508

Energy bands and phonon dispersion for 2D Nb_2C and calculation details (PDF)

AUTHOR INFORMATION

Corresponding Author

*zmsun@buaa.edu.cn

ORCID

Zhimei Sun: 0000-0002-4438-5032

Notes

The authors declare no competing financial interest.

ACKNOWLEDGMENTS

This work is financially supported by the National Key Research and Development Program of China (Grant No. 2017YFB0701700) and the National Natural Science Foundation of China (No. 51871009).

REFERENCES

(1) Lindsay, L.; Broido, D. A.; Reinecke, T. L. Thermal Conductivity and Large Isotope Effect in GaN from First Principles. *Phys. Rev. Lett.* **2012**, *109*, 095901.

(2) Lindsay, L.; Broido, D. A.; Mingo, N. Lattice thermal conductivity of single-walled carbon nanotubes: Beyond the relaxation time approximation and phonon-phonon scattering selection rules. *Phys. Rev. B: Condens. Matter Mater. Phys.* **2009**, *80*, 125407.

(3) Lindsay, L.; Broido, D. A.; Mingo, N. Flexural phonons and thermal transport in multilayer graphene and graphite. *Phys. Rev. B: Condens. Matter Mater. Phys.* **2011**, *83*, 235428.

(4) Cai, Y.; Lan, J.; Zhang, G.; Zhang, Y.-W. Lattice vibrational modes and phonon thermal conductivity of monolayer MoS 2. *Phys. Rev. B: Condens. Matter Mater. Phys.* **2014**, *89*, 035438.

(5) Guo, Z.; Miao, N.; Zhou, J.; Pan, Y.; Sun, Z. Coincident modulation of lattice and electron thermal transport performance in MXenes via surface functionalization. *Phys. Chem. Chem. Phys.* **2018**, *20*, 19689−19697.

(6) Liao, B.; Qiu, B.; Zhou, J.; Huberman, S.; Esfarjani, K.; Chen, G. Significant Reduction of Lattice Thermal Conductivity by the Electron-Phonon Interaction in Silicon with High Carrier Concentrations: A First-Principles Study. *Phys. Rev. Lett.* **2015**, *114*, 115901.

(7) Wang, T.; Gui, Z.; Janotti, A.; Ni, C.; Karandikar, P. Strong effect of electron-phonon interaction on the lattice thermal conductivity in 3C-SiC. *Physical Review Materials* **2017**, *1*, 034601.

(8) Campi, D.; Paulatto, L.; Fugallo, G.; Mauri, F.; Bernasconi, M. First-principles calculation of lattice thermal conductivity in crystalline phase change materials: GeTe, Sb 2 Te 3, and Ge 2 Sb 2 Te 5. *Phys. Rev. B: Condens. Matter Mater. Phys.* **2017**, *95*, 024311.

(9) Wang, Y.; Lu, Z.; Ruan, X. First principles calculation of lattice thermal conductivity of metals considering phonon-phonon and phonon-electron scattering. *J. Appl. Phys.* **2016**, *119*, 225109.

(10) Tong, Z.; Bao, H. Decompose the electron and phonon thermal transport of intermetallic compounds NiAl and Ni3Al by first-principles calculations. *Int. J. Heat Mass Transfer* **2018**, *117*, 972−977.

(11) Maksimov, E.; Shulga, S. Nonadiabatic effects in optical phonon self-energy. *Solid State Commun.* **1996**, *97*, 553−560.

(12) Bianchi, M.; Rienks, E. D. L.; Lizzit, S.; Baraldi, A.; Balog, R.; Hornekær, L.; Hofmann, P. Electron-phonon coupling in potassium-doped graphene: Angle-resolved photoemission spectroscopy. *Phys. Rev. B: Condens. Matter Mater. Phys.* **2010**, *81*, 041403.

(13) Saitta, A. M.; Lazzeri, M.; Calandra, M.; Mauri, F. Giant Nonadiabatic Effects in Layer Metals: Raman Spectra of Intercalated Graphite Explained. *Phys. Rev. Lett.* **2008**, *100*, 226401.

(14) Lin, H.; Gao, S.; Dai, C.; Chen, Y.; Shi, J. A Two-Dimensional Biodegradable Niobium Carbide (MXene) for Photothermal Tumor Eradication in NIR-I and NIR-II Biowindows. *J. Am. Chem. Soc.* **2017**, *139*, 16235−16247.

(15) Mohammad, K.; Masao, A.; Taizo, S.; Chan-Yeup, C.; S, V. N.; Mehdi, E.; Yoshio, S.; Yoshiyuki, K. Novel Electronic and Magnetic Properties of Two-Dimensional Transition Metal Carbides and Nitrides. *Adv. Funct. Mater.* **2013**, *23*, 2185−2192.

(16) Kumar, S.; Schwingenschlögl, U. Thermoelectric performance of functionalized Sc_2C MXenes. *Phys. Rev. B: Condens. Matter Mater. Phys.* **2016**, *94*, 035405.

(17) Gandi, A. N.; Alshareef, H. N.; Schwingenschlgl, U. Thermoelectric Performance of the MXenes M2CO2 (M = Ti, Zr, or Hf). *Chem. Mater.* **2016**, *28*, 1647−1652.

(18) Bai, L.; Yin, H.; Wu, L.; Zhang, X. First-principle study of the Nbn+1CnT2 systems as electrode materials for supercapacitors. *Comput. Mater. Sci.* **2018**, *143*, 225−231.

(19) Tongming, S.; Rui, P.; D, H. Z.; Michael, N.; N, I. I.; Kahk, K. J.; Zuzeng, Q.; Zhanhu, G.; Zili, W. One-Step Synthesis of Nb2O5/C/Nb2C (MXene) Composites and Their Use as Photocatalysts for Hydrogen Evolution. *ChemSusChem* **2018**, *11*, 688−699.

(20) Guo, Z.; Zhou, J.; Zhu, L.; Sun, Z. MXene: a promising photocatalyst for water splitting. *J. Mater. Chem. A* **2016**, *4*, 11446−11452.

(21) Giannozzi, P.; Baroni, S.; Bonini, N.; Calandra, M.; Car, R.; Cavazzoni, C.; Ceresoli, D.; Chiarotti, G. L.; Cococcioni, M.; Dabo, I.; Corso, A. D.; de Gironcoli, S.; Fabris, S.; Fratesi, G.; Gebauer, R.; Gerstmann, U.; Gougoussis, C.; Kokalj, A.; Lazzeri, M.; Martin-Samos, L.; Marzari, N.; Mauri, F.; Mazzarello, R.; Paolini, S.; Pasquarello, A.; Paulatto, L.; Sbraccia, C.; Scandolo, S.; Sclauzero, G.; Seitsonen, A. P.; Smogunov, A.; Umari, P.; Wentzcovitch, R. M. QUANTUM ESPRESSO: a modular and open-source software project for quantum simulations of materials. *J. Phys.: Condens. Matter* **2009**, *21*, 395502.

(22) Kresse, G.; Hafner, J. Ab initio molecular dynamics for open-shell transition metals. *Phys. Rev. B: Condens. Matter Mater. Phys.* **1993**, *48*, 13115−13118.

(23) Li, W.; Carrete, J.; Katcho, N. A.; Mingo, N. ShengBTE A solver of the Boltzmann transport equation for phonons. *Comput. Phys. Commun.* **2014**, *185*, 1747−1758.

(24) Poncíę, S.; Margine, E.; Verdi, C.; Giustino, F. EPW: Electron-Cphonon coupling, transport and superconducting properties using maximally localized Wannier functions. *Comput. Phys. Commun.* **2016**, *209*, 116−133.

(25) Methfessel, M. M.; Methfessel; Paxton, A. T. *Phys. Rev. B: Condens. Matter Mater. Phys.* **1989**, *40*, 3616. de Montigny, M.; Marleau, L. *Phys. Rev. D: Part. Fields* **1989**, *40*, 3616.

(26) Carrete, J.; Li, W.; Lindsay, L.; Broido, D. A.; Gallego, L. J.; Mingo, N. Physically founded phonon dispersions of few-layer materials and the case of borophene. *Mater. Res. Lett.* **2016**, *4*, 204−211.

(27) McWhan, D.; Remeika, J.; Maita, J.; Okinaka, H.; Kosuge, K.; Kachi, S.; Mahan, G. D. *Many-Particle Physics*, 2nd ed.; Plenum Press: New York, 1990. Maier, T.; Jarrell, M. *Phys. Rev. B: Condens. Matter Mater. Phys.*, **2002**, *65*, 041104. Maier, T., Jarrell, M.; Pruschke, T.; Keller, J. *Phys. Rev. Lett.*, **2000**, *86*, 1524. Mattheiss, L. F. *Phys. Rev. B*, **1972**, *5*, 290. *Phys. Rev. B* **1973**, *7*, 326.

(28) Grimvall, G. *The Electron−Phonon Interaction in Metals*; North-Holland Publishing Co. 1981; Vol. *16*, p 304.

(29) Caruso, F.; Hoesch, M.; Achatz, P.; Serrano, J.; Krisch, M.; Bustarret, E.; Giustino, F. Nonadiabatic Kohn Anomaly in Heavily Boron-Doped Diamond. *Phys. Rev. Lett.* **2017**, *119*, 017001.

(30) Butler, W. H.; Pinski, F. J.; Allen, P. B. Phonon linewidths and electron-phonon interaction in Nb. *Phys. Rev. B: Condens. Matter Mater. Phys.* **1979**, *19*, 3708−3721.

(31) Gillis, N. S. Self-Consistent Phonons and the Coupled Electron-Phonon System. *Phys. Rev. B* **1970**, *1*, 1872−1876.

(32) Jain, A.; McGaughey, A. J. H. Strongly anisotropic in-plane thermal transport in single-layer black phosphorene. *Sci. Rep.* **2015**, *5*. DOI: 10.1038/srep08501

(33) Giustino, F. Electron-phonon interactions from first principles. *Rev. Mod. Phys.* **2017**, *89*, 015003.

DOI: 10.1021/jacs.9b01742
J. Am. Chem. Soc. 2019, 141, 8503−8508

(34) Engelsberg, S.; Schrieffer, J. R. Coupled Electron-Phonon System. *Phys. Rev.* **1963**, *131*, 993−1008.
(35) Li, C.; Ravichandran, N. K.; Lindsay, L.; Broido, D. Fermi Surface Nesting and Phonon Frequency Gap Drive Anomalous Thermal Transport. *Phys. Rev. Lett.* **2018**, *121*, 175901.
(36) Bazhirov, T.; Noffsinger, J.; Cohen, M. L. Superconductivity and electron-phonon coupling in lithium at high pressures. *Phys. Rev. B: Condens. Matter Mater. Phys.* **2010**, *82*, 184509.
(37) Qiu, B.; Tian, Z.; Vallabhaneni, A.; Liao, B.; Mendoza, J. M.; Restrepo, O. D.; Ruan, X.; Chen, G. First-principles simulation of electron mean-free-path spectra and thermoelectric properties in silicon. *EPL (Europhysics Letters)* **2015**, *109*, 57006.
(38) Ziman, J.M. *Electrons and Phonons: The Theory of Transport Phenomena in Solids*; Clarendon Press: Oxford, 1960.
(39) Omini, M.; Sparavigna, A. An iterative approach to the phonon Boltzmann equation in the theory of thermal conductivity. *Phys. B* **1995**, *212*, 101−112.
(40) Feng, T.; Ruan, X. Four-phonon scattering reduces intrinsic thermal conductivity of graphene and the contributions from flexural phonons. *Phys. Rev. B: Condens. Matter Mater. Phys.* **2018**, *97*, 045202.

DOI: 10.1021/jacs.9b01742
J. Am. Chem. Soc. 2019, 141, 8503−8508